Roots Characteristics of a flexible and mature vegetation: Preliminary results of experimental investigation in a meandering laboratory flume

Donatella Termini[1] , *Alice* Di Leonardo[1]

[1]*Dipartimento di Ingegneria Civile, Ambientale, Aerospaziale, dei Materiali (DICAM), 90128 Palermo, Italy*

Abstract. Vegetation controls sediment dynamics and affects the kinematic characteristics of flow in rivers. The uprooting mechanism is strongly affected by mechanical properties, morphology and branching of the roots system. This work presents preliminary results of experimental work conducted in a laboratory meandering flume. The work aims to investigate how the geometrical and mechanical characteristics of the roots of a real, flexible and mature vegetation could vary along the bend. Results show that both the geometrical and the mechanical characteristics of the roots assume higher/lower values in peculiar sections of the bend suggesting that they could be affected by the kinematic characteristic of flow.

1. Introduction

As it is known, the presence of vegetation strongly affects river's evolution processes. In fact, on one hand vegetation influences the kinematics characteristics of the flow, on the other hand, through the roots system, vegetation contributes to limit the erodibility of the river boundaries [1,2]. In turn, the flow could influence the growth and distribution of the vegetation causing, especially during floods, either its uprooting or its mechanical damage [4]. Flow/vegetation interaction processes are influenced by several factors which could be linked both to hydrological phenomena (frequency, duration and magnitude of floods) and to physical and mechanical characteristics of soil (typology and composition) and of vegetation (stiffness, concentration, age).

Especially in recent years, researchers devoted their attention to the uprooting process of vegetation. Perona et al. [3] conducted laboratory experiments to investigate the effect of flood disturbances on the uprooting mechanism. They observed that, especially in the case of frequent flood disturbances, the uprooting mechanism could involve the entire germinated biomass. Other researchers analysed the uprooting mechanism for different conditions of soil, vegetation species and roots systems. In [4] the influence of the age of vegetation on the roots resistance was explored. Authors verified that the uprooting mechanism is different between young vegetation and mature vegetation. Other studies [5, 6, 7] focused on the influence of the soil shear strength on roots resistance and verified that it is strongly affected by the roots system branching. Bailey et al. [8] conducted laboratory

experiments to investigateg the role of multiple roots on the anchorage strength. Karrenberg et al. [9] investigated the roots resistance of different vegetation species. A common result of these studies was that the uprooting mechanism can be strongly affected by the mechanical properties, morphology and branching of the roots system.
In the present work we explore the geometrical and mechanical characteristics of the roots of a mature vegetation and how these characteristics might vary along a meandering bend, where the channel's curvature changes in stream-wise direction modifying the kinematic characteristics of flow. The analysis is carried out in a laboratory flume constructed at the laboratory of the Dipartimento di Ingegneria Civile, Ambientale, Aerospaziale e dei Materiali (DICAM) – University of Palermo (Italy).

2. Experimental apparatus and procedure

The experimental run considered in the present work was conducted in a sine-generated meandering flume of large amplitude ($\theta_0 = 110°$). The channel's cross-section is rectangular with width $B = 0.50$ m and length at the channel axis is $L = 28$ m. In this work, attention is restricted to the measurement sections (1, 2, 3, 4 and 5) shown on Fig. 1a. The flume is equipped by a submersible pump (type Flygt 3085-183) that allows to convey the flow at the upstream boundary through a recirculating system (see Fig.1a). The bed follows the equilibrium configuration obtained at the end of a mobile-bed run conducted as described in [10, 11]. Furthermore, the bed is uniformly covered by mature vegetation (see Fig.1b), which was obtained as natural growth state of the young flexible vegetation (*Festuca arundinacea* - concentration of 200 $stems/dm^2$ - see in [10, 11]), previously installed on the deformed bed to conduct the experimental runs (with a constant water discharge of 0.012 m^3/s) described in [12, 13].

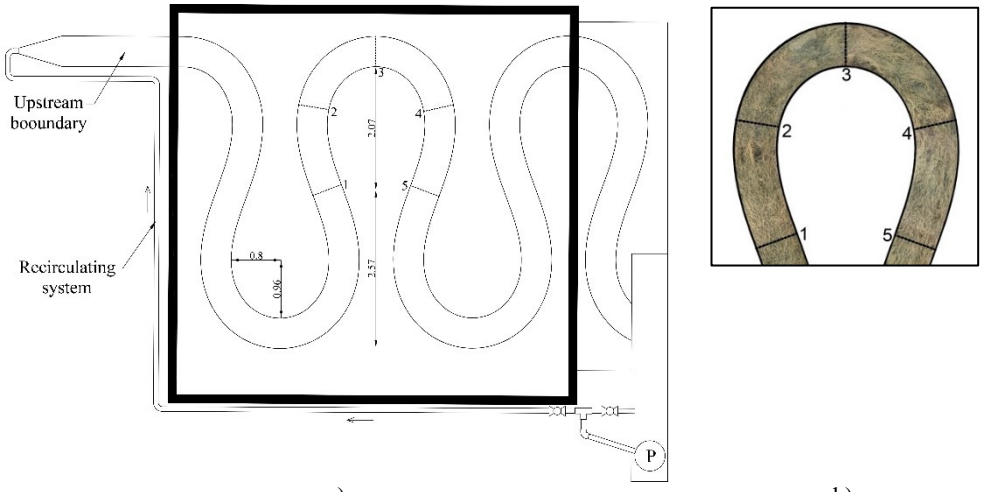

Fig.1. a) Plane-view of the experimental apparatus; b) Examined bend covered by mature vegetation

In order to investigate the variation of the geometrical and mechanical characteristics of the roots system along the bend two samples of vegetation were extracted close to the banks of each examined section (see Fig.2a); for each sample, 10 roots were examined. The geometrical characteristics (length and thickness) of the roots were measured by

considering the reference system x,y,z of Fig.2a (with y-axis along the section, x-axis perpendicular to y-axis, z-axis along the vertical direction). The roots length was measured by using calibrated photos, acquired with a high resolution camera (Nikon-24 Mp) along the $x-z$ plane. The roots thickness was measured by using a digital calliper (accuracy of 0.01 mm).

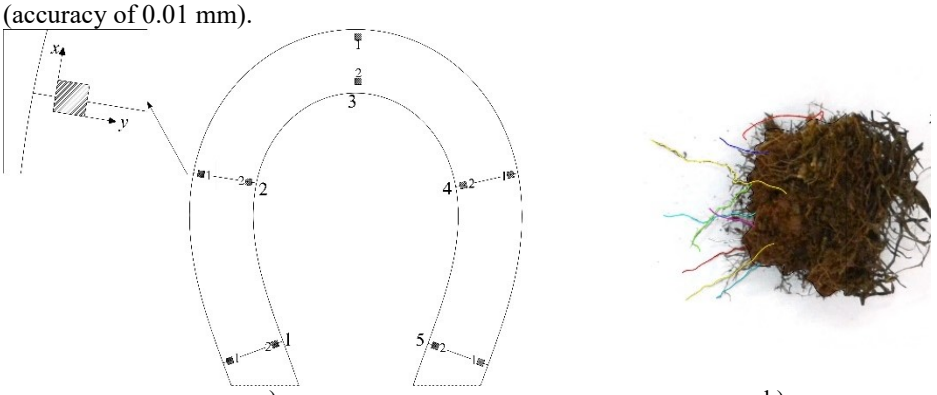

a) b)

Fig. 2. a) Reference system and positions of the extracted samples; b) Picture of the sample extracted by the vegetated bed close to the outer bank of the section 4

In order to evaluate the roots mechanical characteristics, the extracted roots were subjected to a tensile test by using the testing machine (by Zwick/Roell - see Fig.3) located at the Materials laboratory of DICAM. This machine is equipped with a load cell of 5 kN (resolution of 0.01 N). The roots were hold by the two clamps of the testing machine at a mutual distance of 10 mm (see Fig.3). It was set a pretension of 0.03 N and a pulling velocity of 1 mm/min.

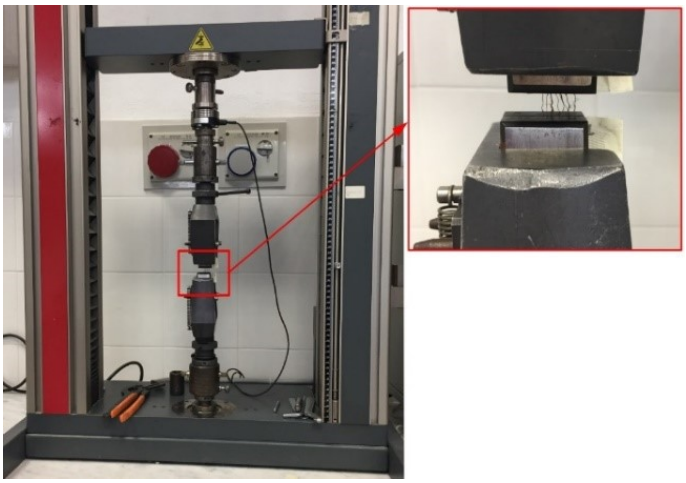

Fig.3. Photo of the testing machine used with the particular of the clamping of a sample

The software of the testing machine allows plotting the stress σ_T (expressed in N/mm^2) against the roots deformation, ε (expressed in percentage with respect to the initial distance between the two clamps). As an example, in Fig.4 the graph σ_T-ε, obtained for the roots of the sample extracted near the outer bank of section 2, is shown. It can be

observed that, in the first phase, the values ($\sigma_T - \varepsilon$) follow a linear trend (elastic phase). The angular coefficient of the linear equation $\sigma_T - \varepsilon$ obtained in this phase has allowed us to estimate the Young's modulus, *E*, that is related to the roots stiffness (see Fig. 4). After the reaching of a maximum value, σ_T decreases in value and the graph $\sigma_T - \varepsilon$ presents different jumps, each corresponding to the breakage of a single root.
The resistance force, F (expressed in *N*), was obtained by multiplying the stress σ_T for the total transversal section of the roots (A_r) which was obtained, by approximating each root to a cylinder with diameter equal to the corresponding thickness, S_r , as:

$$A_r = \sum_{i=1}^{n_{tr}} \pi \times \frac{S_{r,i}^2}{4} \qquad i = 1....10 \tag{1}$$

The graph $F - \varepsilon$ was also plotted for each sample.

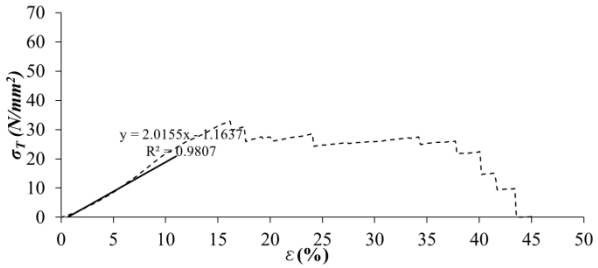

Fig.4. Graph σ_T - ε for the sample extracted near the outer bank of section 2

3. Results

3.1. Roots geometrical characteristics

By using the measured values, the mean roots length, $\overline{L_r}$, and the mean roots thickness, $\overline{S_r}$, were evaluated for each sample as:

$$\overline{L_r} = \frac{\sum_{i}^{n_r} L_{r,i}}{n_r} \; ; \quad \overline{S_r} = \frac{\sum_{i}^{n_r} S_{r,i}}{n_r} \; ; \tag{2}$$

By estimating the standard deviations of the lengths and the thickness of the roots as:

$$\sigma_L = \sqrt{\frac{\sum_{i=1,n_r} \left(L_{r,i} - \overline{L_r}\right)^2}{n_r}} \quad ; \quad \sigma_{S_r} = \sqrt{\frac{\sum_{i=1,n_r} \left(S_{r,i} - \overline{S_r}\right)^2}{n_r}} \tag{3}$$

it was possible to evaluate that the uncertainty in averaging the roots length was less than 20% and the uncertainty in averaging the roots thickness was less than 2%
Fig. 5 reports the values of $\overline{L_r}$ (Fig. 5a) and of $\overline{S_r}$ (Fig. 5b) obtained for each extracted sample. From this figure it can be observed that, along the outer bank, the mean roots length, $\overline{L_r}$, assumes low values at sections 1 and 2, then $\overline{L_r}$ increases in value until to reach

section 3 where the maximum value is reached; then $\overline{L_r}$ decreases again until section 5. Along the inner bank, $\overline{L_r}$ assumes an increasing trend until section 2 where the maximum value is obtained; it decreases until a minimum at section 3 and then it increases again until to reach section 5. Thus, the trend of $\overline{L_r}$ along the outer bank is opposite to that obtained along the inner bank.

The mean roots thickness, $\overline{S_r}$, (Fig.5b) increases along the outer bank until a maximum at section 2; then it decreases until a minimum at section 4 and increases again until section 5; along the inner bank, $\overline{S_r}$ slightly decreases until section 2 and then it increases until section 5.

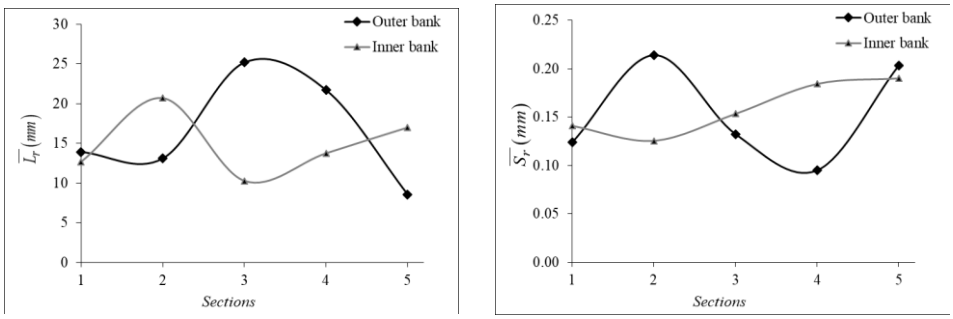

a) b)

Fig.5. Values estimated for each extracted sample: a) mean roots length $\overline{L_r}$ (mm); b) mean roots thickness $\overline{S_r}$ (mm)

3.2. Roots mechanical characteristics

Similarly to what observed for the graphs $\sigma_T - \varepsilon$, the graphs $F - \varepsilon$ presented, after the elastic phase, a maximum value of the resistance force (F_{max}). As an example, Fig.6a reports the graph $F - \varepsilon$ for the sample extracted near the outer bank of section 2. In this figure the *i*-th jump of the resistance force is $F_{p,i}$. By considering the number of jumps n_p the value:

$$F_{max,m} = F_{max} / n_p \tag{4}$$

has been considered as the representative value of the resistance force of the roots system.

Fig.6b shows the value of $F_{max,m}$ obtained along the inner and the outer banks of each examined section. From this figure it can be observed that, along the outer bank, $F_{max,m}$ assumes low values at the inflection sections (sections 1 and 5) and at the apex section (section 3); it assumes a maximum at section 2 (bend entrance) and a second peak value at section 4 (bend exit). Along the inner bank, $F_{max,m}$ decreases up to section 2, where there is a minimum; then it increases until to obtain a maximum value at section 4; finally, it decreases again until to reach section 5.

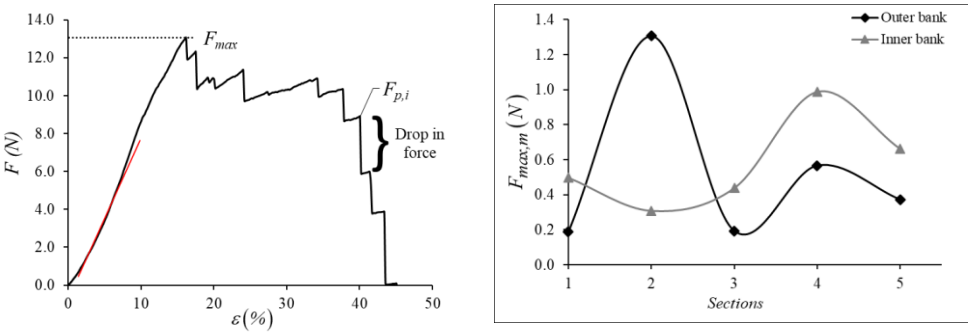

Fig.6. a) Trend of the force F varying the deformation ε for the sample extracted near the outer bank of section 2; b) Values of $F_{max,m}$ along the bend

4. Discussion

The results reported in the previous section 3 demonstrate that the geometrical and the mechanical characteristics of the roots system vary along the meandering bend.
The relation between the variation of the mechanical characteristics and that of the geometrical characteristics can be examined from Figure 7 which reports the estimated values of the representative resistance force, $F_{max,m}$, against the mean roots length, $\overline{L_r}$, and the mean roots thickness, $\overline{S_r}$, along the bend.

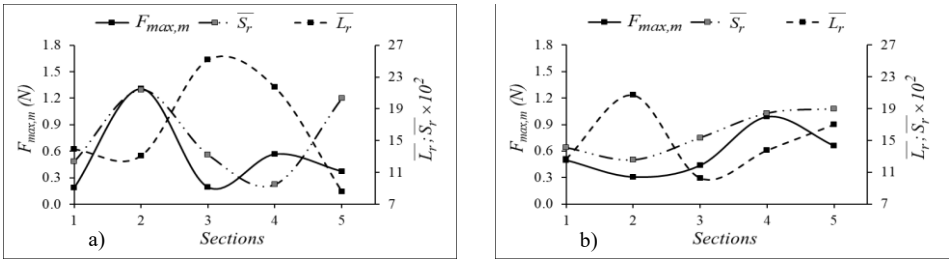

Fig.7. a) Comparison between $F_{max,m}$, $\overline{L_r}$ and $\overline{S_r}$ along the outer bank; b) Comparison between $F_{max,m}$, $\overline{L_r}$ and $\overline{S_r}$ along the inner bank

Figure 7 shows that, along both banks, $F_{max,m}$ assumes a trend opposite to that of $\overline{L_r}$ and similar to that of $\overline{S_r}$. This means that, generally, the roots characterized by high resistance are those characterized by high thickness and low length. Thus (see Figure 7) the samples extracted close to the outer bank of section 2 (bend entrance) and close to the inner bank of section 4 (bend exit) are characterized by short and large roots and by high resistance force. At the apex section (section 3), the roots extracted close to the outer bank are characterized by roots longer and thinner than those extracted close to the inner bank; the resistance force of the roots close to the outer bank is lower than that of the roots close to the inner bank. At the inflection sections (sections 1 and 5) the difference in the resistance force between the outer and the inner banks is less evident.
Termini [10] conducted experiments in the same channel as that considered in the present work and verified that the maximum flow velocity moves at the outer bank at the entrance of the bend (i.e. at section 2) and then the flow accelerates; downstream of the apex section, approaching the bend exit (i.e. at section 4) the flow convectively decelerates. Thus, the obtained results suggest that the variation of the geometrical and the mechanical

characteristics of the roots along the bend could be strongly related to the variation of the kinematic characteristics of the flow. This is also confirmed from Fig. 8, where the values of $\overline{L_r}$, and $\overline{S_r}$, are compared with those of the water depths measured along the outer bank during the experimental runs [12, 13]. Figure 8 shows that the trend of h is similar to that of $\overline{L_r}$.

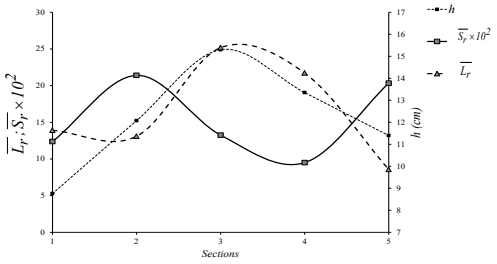

Fig. 8. Comparison between $\overline{S_r}$ and $\overline{L_r}$ and the water depth h along the outer bank

The variation of the resistance force along the bend is also related to the variation of the roots stiffness. This behaviour can be examined from Fig. 9 which compares the resistance force, $F_{max,m}$, to the estimated Young's modulus E along the bend. It can be noted that, passing from section 1 to section 2, E decreases along the outer bank and is almost constant along the inner bank while $F_{max,m}$ increases along the outer bank and slightly decreases along the inner bank; passing from section 2 to section 3, both E and $F_{max,m}$ decrease along the outer bank while along the inner bank $F_{max,m}$ increases and E slightly decreases. Thus, passing from the inflection section to the bend entrance (section 2), along the outer bank, the trend of E is different to that of $F_{max,m}$. Downstream of the apex (section 3), E and $F_{max,m}$ show a similar trend along both the channel banks. Thus from Fig. 9 it can be concluded that the roots characterized by the highest resistance force are those extracted close to the outer bank of the bend entrance (section 2). A second lower peak value of the resistance force is found close to the outer bank of the section 4 (bend exit); these roots are characterized by the highest values of the Young modulus.

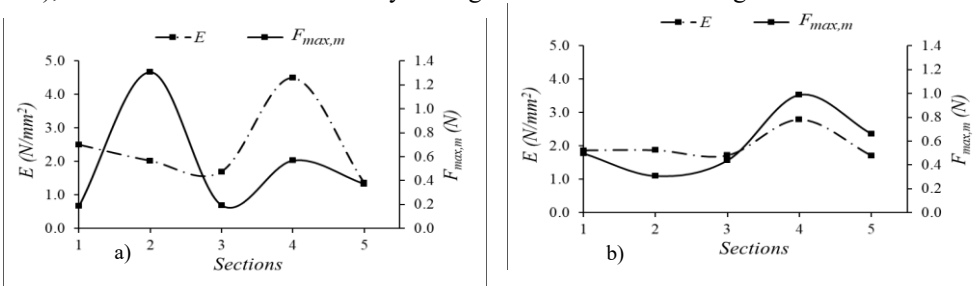

Fig.9. Comparison between E and $F_{max,m}$: a) along the outer bank; b) along the inner bank

5. Conclusion

An experimental study has been recently conducted at the laboratory of the Dipartimento di Ingegneria Civile, Ambientale, Aerospaziale e dei Materiali (DICAM) – University of

Palermo (Italy) in order to evaluate the variation of the geometrical and mechanical characteristics of a real, mature and flexible vegetation in a meandering bend.
The results demonstrate that the characteristics of the vegetation vary along the bend of the meandering channel. Generally, the roots characterized by high resistance are those characterized by high thickness and low length. In particular, it has been observed that the roots characterized by the highest resistance force are those extracted close to the outer bank of the bend entrance (section 2); these roots are also more rigid (i.e. characterized by the low values of the Young modulus, E). A second lower peak value of the resistance force has been observed close to the outer bank of the section 4 (bend exit), but these roots are characterized by the highest values of the Young modulus.
Thus, the obtained results suggest that the geometrical and the mechanical characteristics of the roots system could vary along the bend as function of the variation of the kinematic characteristics of the flow. This behaviour will be investigated in a successive work.

REFERENCES

1. Corenblit D., Tabacchi E., Steiger J., Gurnell A., *Reciprocal interactions and adjustments between fluvial landforms and vegetation dynamics in river corridors: A review of complementary approaches*, Earth Sci. Rev. **84**, 56–86 (2007)
2. Murray A., Knaapen M., Tal M., Kirwan M., *Biomorphodynamics: Physical-biological feedbacks that shape landscapes*, Water Resour. Res. **44**, W11301 (2008)
3. Perona P., Molnar P., Crouzy B., Perucca E., Jiang Z., McLelland S., Wuthrich D., Edmaier K., Francis R., Camporeale C., Gurnell A., *Biomass selection by floods and related timescales: Part 1. Experimental observations*, Adv. Water Resour. **39**, 85-96 (2012)
4. Edmaier K., Burlando P., Perona P., *Mechanisms of vegetation uprooting by flow in alluvial non-cohesive sediment,* Hydrol. Earth Syst. Sci. **15**, 1615-1627 (2011)
5. Pollen N., *Temporal and spatial variability in root reinforcement of streambanks: Accounting for soil shear strength and moisture*, Catena **69**, 197-205 (2007)
6. Ennos A.R., *The anchorage of leek seedlings: The effect of root length and soil strength*, Ann. Bot. **65**, 409-416 (1990)
7. Schwarz M., Cohen D., Or D., *Pullout tests of root anchorage and natural bundles in soil: Experiments and modelling,* J Geophys Res **116**, F02007 (2011)
8. Bailey P., Currey J., Fitter A., *The role of root system architecture and root hairs in promoting anchorage against uprooting forces in allium cepa and root mutants of arabidopsis thaliana*, J. Exp. Bot. **53**, 333-340 (2002)
9. Karrenberg S., Blaser S., Kollmann J., Speck T., Edwards P., *Root anchorage of saplings and cuttings of woody pioneer species in a riparian environment,* Funct. Ecol. **17**(2), 170-177 (2003)
10. Termini D., *Experimental observations of Flow and Bed processes in a Large-amplitude Meandering Flume"*. Journal of Hydraulic Engineering – **135**(7), 575-587, (2009).
11. Termini D., Piraino M., *Experimental analysis of cross-sectional flow motion in a large amplitude meandering bend*, Earth Surf. Process. Landf. **36**(2), 244–256 (2011)
12. Termini D., *Experimental analysis of the effect of vegetation on flow and bed shear stress distribution in high-curvature bends*, Geomorphology **274**, 1-10 (2016).
13. Termini D., *Vegetation effects on cross-sectional flow in a large amplitude meandering bend.* Journal of Hydraulic Research. **55**(3). 423-429 (2017).